Simultaneous Active and Passive SAR imaging – first results

Damian Gromek, Piotr Samczyński, Krzysztof Radecki, Jędrzej Drozdowicz, Krzysztof Stasiak
Institute of Electronic Systems
Warsaw University of Technology
Warsaw, Poland
dgromek@elka.pw.edu.pl

***Abstract*—Synthetic Aperture radar (SAR) is widely used for Earth ground imaging and mapping. In most cases, the SAR radar is an active device and can be mounted on both air- and space-borne platforms. Passive SAR imagery utilizes different illuminators of opportunity such as DVB-T, WIFI, or other active radar transmitters has been gaining attention recently. In results first experimental results of passive SAR imaging have been shown in last years by researchers. Simultaneous active and passive SAR imaging is the next natural step in the development of this technology. In this paper, a system which consists of two demonstrators operates together in active (C band) and passive (DVB-T band) modes is presented. The preliminary results of the active and passive SAR imaging of the same ground area taken at the same time using a small airborne platform have been shown.**

Keywords—SAR imaging, Active SAR, Passive SAR, ground imaging, passive radar,

I. Introduction

Active SAR technology has been well known since the early 1950s, and is widely used in many civilian and military applications [1]. The active radar has many advantages, i.e. the geometry is monostatic, the signal used is specially designed for radar imaging purposes, and the transmitter and receiver are synchronized. Additionally, active SAR systems use well-known techniques of signal processing which are easy to implement and operate in real time. At this stage of development, active SAR has many advantages over passive, especially for civilian applications. The most important are the high resolution (up to centimeters) of the acquired SAR images, it doesn't depend on external emissions, the processing of data is fast, and the results are obtained automatically. Passive SAR might be an attractive novel solution in military applications because it doesn't have its own emission, so it is hard to detect such a system by electromagnetic radiation. However, passive imaging might also find applications in civilian radar imaging, where high-resolution imaging is not greatly required. For example, the relatively low-resolution SAR images (tens of meters in resolution) provided by space-based Sentinel SAR instruments are effectively used in many geodesy applications [2]. In the future, passive SAR imaging might become a low-cost alternative to the low-resolution, space-based SAR systems widely used in civilian applications.

Passive SAR imaging in the bistatic configuration is not a new concept, but up to the beginning of the 21st century it was not widely considered [3-6]. Nowadays, it is under investigation due to the availability of high amount of illuminators of opportunity such as GSM, LTE, WIFI, FM, and DVB-T, among others. It caused that the occupied bandwidth is getting wider, so the resolution can be better, reaching even single meters (e.g. up to 4 meters when using for 5 DVB-T adjacent channels) in passive SAR imaging [7]. What's more, there are effective possible today to implement in real-time digital signal processing techniques to suppress the direct echo cancellation [8], which was one of the main problems in passive radars. Some interesting results, especially using DVB-T illumination, have been shown over the last decade [9-13]. The concept of combining results from two SAR systems – active and passive operating at the same time and observing the same region of interest – is novel and can bring additional benefits in future by allowing the fusion of SAR images obtained using those two technologies. The first results of active/passive SAR imaging operating in UHF-band has been shown in [14]. Additionally when operating on different frequencies the additional features of the targets can be show in SAR images. Merging images from different sources may develop deeper information about an observed area. The first experiment of collecting active and passive SAR images simultaneously was carried out by the authors in September 2019 during the NATO STO (Science and Technology) measurement campaign named APART-GAS (Active PAssive Radar Trials – Ground-based, Airborne, Seaborne). The trials were organized as joint trials of two NATO SET (Sensor and Technology) RTGs (research task groups): SET-242, which works on Passive Coherent Locators on Mobile Platforms, and SET-258, which works on DMPAR (Deployable multiband passive/active radar) Deployment and Assessment in Military Scenarios. Within the measurement campaign, the authors carried out the experiments using a small Cessna aircraft as a radar carrier, on which two SAR systems were mounted: an active SAR system operating in 5.3 to 5.7 GHz (C band), and a passive SAR which covered a wide DVB-T frequency range: from 150 MHz up to 900MHz. The passive radar receiver was capable of recording up to 50 MHz of bandwidth simultaneously in the reference and surveillance channels. The first results from this measurement campaign are presented in this paper.

II. System description

A. Active SAR component

The active SAR used in the experiment was a C-band radar demonstrator built by the researchers from the Warsaw University of Technology (WUT) [15]. The demonstrator is highly integrated and is a standalone device which is configured and managed over an Ethernet connection. The enclosure was specially designed to provide external electromagnetic radiation immunity. The picture of developed demonstrator is presented in Figure 1. It is an FMCW (Frequency Modulation Continuous Wave) radar with two antennas (only one is visible in the figure): one for

978-83-949421-5-1 ©2020 Warsaw University of Technology

transmission and one for echo signal reception. The main parameters of the system are presented in Table I. The demonstrator integrated on the Cessna platform used in the experiment is shown in Fig. 2 and Fig. 3.

Figure 1: C-band radar designed by WUT a) - CAD model b) - real photograph – only one antenna (Rx) is installed and presented.

TABLE I. C-BAND RADAR MAIN PARAMETERS

Operating band	5 – 6 GHz
Carrier frequency	5.52 Ghz
Bandwidth	24 – 480 MHz
PRF	0.1-2 kHz
Emitted power	100 mW
Elevation beamwidth	20^0
Azimuth beamwidth	20^0
Range resolution	30 cm
Cross-range resolution	30 cm
Power consumption	80 Watt
Weight	5 kg
Dimensions	13 cm x 17 cm x 38 cm

B. *Passive SAR component*

The passive SAR demonstrator used in the experiment was constructed from Commercial Off-The-Shelf (COTS) components, that is: a CUDA NVIDIA Jetson AGX Xavier [16] as a recording and processing unit, a USRP X310 as a fast Analog-to-Digital converter capable of acquiring 50 MHz of bandwidth in two receiving paths (reference and surveillance), a GPS sensor for positioning, and DVB-T home indoor antennas. The system is presented in Figure 3.

The Jetson AGX Xavier [16] supports Compute Unified Device Architecture (CUDA) for parallel computing. The internal storage memory is only 32GB, but the NVMe connector gives the ability to mount additional fast SSD storage. The PCIe connector is used to mount a 10Gb Ethernet adapter for communication with the USRP device, as the built-in Ethernet link is used to control the whole passive SAR component.

In Table II the main parameters of the passive SAR radar demonstrator are presented. The Passive SAR demonstrator is capable to acquire up to 5 adjacent DVB-T Channels (50 MHz) in two receiving paths, in real time. This could provide the resolution of 4 m in the range direction and the quasi-monostatic case. Due to the low density of the DVB-T spectrum in Poland, the authors conducted the experiments with a maximum of 2 DVB-T channels. For the georeferencing of the produced SAR images, a GPS platform was also integrated in the demonstrator. The antennas used in the experiment were standard DVB-T antennas.

TABLE II. DVB-T PASSIVE SAR RADAR MAIN PARAMETERS

Operating band	10 – 1000 MHz
Bandwidth	up to 50 MHz @ ref & surv
Range resolution	20 m (1 CH), 4 m (5 CH)
Cross-range resolution	depends on integration time
Power consumption	75 Watt
Weight (Xavier + USRP)	~2.5 kg
Dimensions	27.7 cm x 21.8 cm x 3.9 cm (USRP) 10.5 cm x 10.5 cm x 6.5 cm (Xavier)

Figure 2: Active and Passive SAR system on Cessna aircraft

Figure 3: View inside the cockpit, Passive SAR system - on top of the main rack, Active SAR - at the bottom

III. SAR PROCESSING

A. Active SAR processing

The active SAR imaging algorithm used to process the data in the carried out experiment is based on the focused SAR technique [17]. In the first step, the range compression is performed using fast Fourier transform (FFT). Then the estimated trajectory of the radar platform is obtained with the MapDrift autofocus algorithm [18-19]. Finally, the azimuth compression with the matched filter is applied [17]. Figure 4 presents the steps of the active SAR processing.

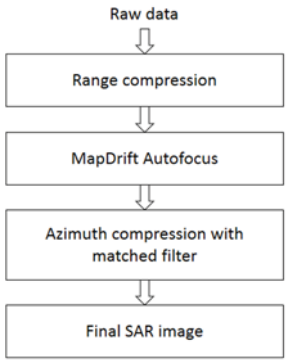

Figure 4: Block diagram of the active SAR processing.

B. Passive SAR processing

To obtain passive SAR images, the cross-correlation function on the reference and surveillance signals is performed at first to obtain range-time matrix for further processing. Furthermore, the fast barycentric back-projection algorithm (BBPA) is used for processing [20]. The main assumption of the BBPA algorithm is the creation of the virtual synthetic beam with its starting point in the reconstructed point. The virtual beam illuminates the flight trajectory, therefore a large amount of calculations is reduced, with a narrowed raw data range used for the image reconstruction [20]. The idea of the virtual synthetic aperture beam is presented in Fig. 5.

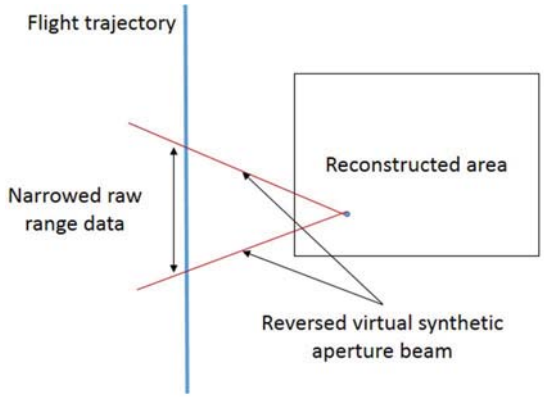

Figure 5: The idea of the virtual synthetic aperture radar in the barycentric-based back projection algorithm

In the further step of the BBPA, the raw data from the illuminated range is integrated as in the classical back projection algorithm [20]. The implementation of the algorithm can be easily parallelized on the Xavier device.

IV. EXPERIMENT SETUP

The experiment using active and passive radar for ground imaging was conducted in September 2019 within the NATO STO APART-GAS trials. The measurement scenario is presented in Figure 6. The DVB-T transmitter of opportunity utilized by the passive radar receiver was placed near Koszalin city, in the village of Gołogóra. The 250 meter tall TV mast used in the experiment was at the ground level of 210 meters above sea level. The ground level of the imaged terrain was 90 meters above sea level at a distance of 25 km from the DVB-T mast. Such bistatic geometry gives an 89.12^0 incidence angle of the DVB-T illumination at the imaged scene. The Cessna aircraft was flying at a constant speed of 40 m/s at an altitude of 300 meters.

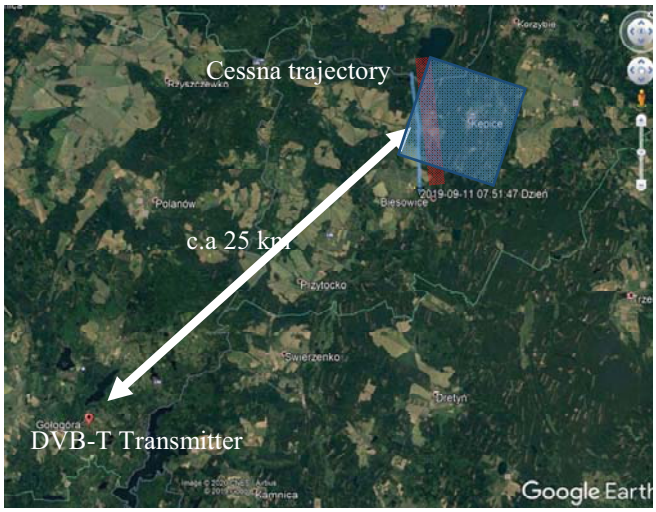

Figure 6: Passive and Active SAR experiment - data acquisition scenario. Imaged region for active and passive SAR marked with red and blue rectangles respectively

V. FIRST RESULTS & CONCLUSIONS

The results obtained from active and passive SAR together with their optical counterpart are presented in Figures 7 and 8 respectively. The radar platform trajectory is indicated by the blue lines. The area covered by the active SAR radar was narrow in the range direction (around 400 meters on the ground) due to the narrow beamwidth of the antenna (20^0) and the low altitude of the flight. Additionally, the very low quality of the image was caused by the issue with the analog front end part of the system. The issue was hard to resolve during the campaign, and this negatively affected the obtained results. For the same area, the passive SAR image could be calculated for a much wider area due to the omnidirectional illumination from the transmitter and the wide beamwidth of the DVB-T antennas used. At first glance, it is very hard to find corresponding parts between active and passive SAR images, due to the different geometry and also different resolutions of both images, and the only partial overlay of each for the same area. The main difference that has a major influence on the SAR images is the aforementioned differences in geometries. In active SAR, the geometry is monostatic and the incident angle from the transmitter was around 45^0 which makes it possible to image ground objects. In passive SAR, the geometry is bistatic and due to the long distance from the transmitter (25

km) in the described experiment, the incident wave is almost horizontal (incident angle equal to 89.1^0). This fact makes it possible to see only very tall objects in passive SAR images, such as trees and trunks in the forest, and this is actually the one component which might be identified in both SAR images. The other fact which makes a difference is the operating bands. In the experiment, the passive SAR utilizes the UHF DVB-T band, whereas in the active SAR the C-band was used. In those two bands, ground targets have different reflectivity characterized by different radar cross-sections (RCS). As this paper presents results of the area imaging with two different systems, the merging of both results is a further step of the work to be done in the future.

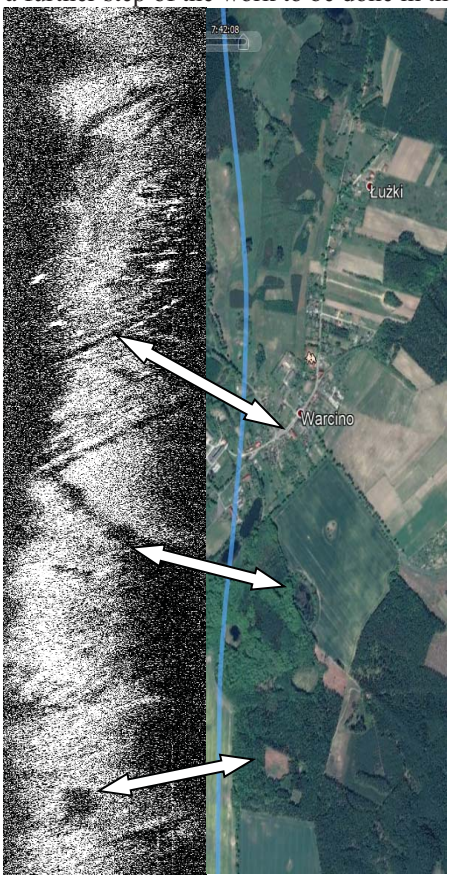

Figure 7: C-band Active SAR radar image (left) and its optical GoogleMap counterpart (right)

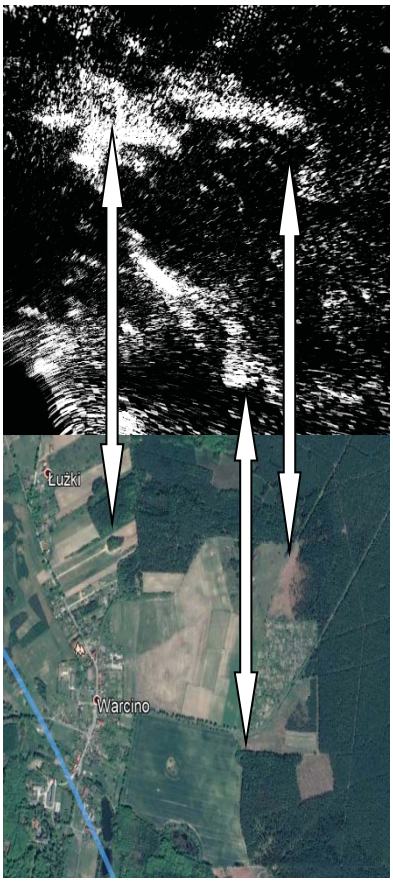

Figure 8: DVB-T Passive SAR image (top) and its optical GoogleMap counterpart (bottom)

ACKNOWLEDGMENT

The authors would like to thank the NATO STO Organization for their support and funds for organizing the APART-GAS trials. Additionally, the authors would like to thank the Air Force Institute of Technology for their involvement in mounting all the system components onboard the Cessna plane; in particular, without the support of Marcin Bryl, Janusz Wiśniewski, and Zbigniew Jakielaszek, the tests in the air would not have been possible.

REFERENCES

[1] Curlander, J.C., McDonough, R.N.: 'Synthetic Aperture Radar. Systems & Signal Processing' (John Wiley & Sons, 1991)

[2] Jaroslaw Wajs, Wojciech J. Milczarek, "Detection of surface subsidence using SAR SENTINEL 1A imagery and the DInSAR method – a case study of the Belchatow open pit mine, Central Poland", E3S Web Conf. 55 00004 (2018), DOI: 10.1051/e3sconf/20175500004

[3] N.J. Willis, and H. Griffiths, Eds., Advances in bistatic radar, SciTech, 2007

[4] G. Yates, A.M. Horne, A.P. Blake, and R. Middleton, "Bistatic SAR image formation," IEE Proceedings - Radar, Sonar and Navigation, vol. 153, no. 3, pp. 208-213, 2006.

[5] P. Dubois-Fernandez, H. Cantalloube, B. Vaizan, G. Krieger, R. Horn, M. Wendler, and V. Giroux, "ONERA-DLR bistatic SAR campaign: planning, data acquisition, and first analysis of bistatic scattering behaviour of natural and urban targets," IEE Proceedings - Radar, Sonar and Navigation, vol. 153, no. 3, pp. 214-223, 2006.

[6] J.H.G. Ender, I. Waltersheid, and A.R. Brenner, "Bistatic SAR - translational invariant processing and experimental results," IEE Proceedings - Radar, Sonar and Navigation, vol. 153, no. 3, pp. 177-183, 2006.

[7] K. Kulpa, M. P. Malanowski, and P. J. Samczyński, "Passive radar: From target detection to imaging," in *Proceedings 2019 IEEE Radar Conference*, 2019.

[8] K. Kulpa, "The CLEAN type algorithms for radar signal processing," *2008 Microwaves, Radar and Remote Sensing Symposium*, Kiev, 2008, pp. 152-157.

[9] L. M. H. Ulander, P. Frölind, A. Gustavsson, R. Ragnarsson and G. Stenström, "VHF/UHF bistatic and passive SAR ground imaging," 2015 IEEE Radar Conference (RadarCon), Arlington, VA, 2015, pp. 0669-0673., doi: 10.1109/RADAR.2015.7131080

[10] L. M. H. Ulander, P. Frölind, A. Gustavsson, R. Ragnarsson and G. Stenström, "Airborne passive SAR imaging based on DVB-T signals," 2017 IEEE International Geoscience and Remote Sensing Symposium (IGARSS), Fort Worth, TX, 2017, pp. 2408-2411., doi: 10.1109/IGARSS.2017.8127477

[11] P. Frölind, "Results of airborne passive SAR ground and sea target imaging using DVB-T signals," 2016 IEEE Radar Conference (RadarConf), Philadelphia, PA, 2016, pp. 1-4. doi: 10.1109/RADAR.2016.7485125

[12] Nithirochananont, U., Antoniou, M., & Cherniakov, M. (2019). Passive multi-static SAR – experimental results.

[13] D. Gromek, K. Kulpa and P. Samczyński, "Experimental Results of Passive SAR Imaging Using DVB-T Illuminators of Opportunity," in *IEEE Geoscience and Remote Sensing Letters*, vol. 13, no. 8, pp. 1124-1128, Aug. 2016, doi: 10.1109/LGRS.2016.2571901.

[14] L. M. H. Ulander, P. Frölind, A. Gustavsson, A. Haglund, R. Ragnarsson and T. Sjögren, "Ground mapping using active and passive UHF-band SAR," 2020 IEEE International Radar Conference (RADAR), Washington, DC, USA, 2020, pp. 524-529, doi: 10.1109/RADAR42522.2020.9114844.

[15] D. Gromek *et al*., "C-band SAR radar trials using UAV platform: Experimental results of SAR system integration on a UAV carrier," *2016 17th International Radar Symposium (IRS)*, Krakow, 2016, pp. 1- 5, doi: 10.1109/IRS.2016.7497305.

[16] Jetson AGX Xavier Developer Kit [Online 20.01.2020]. Available: https://developer.nvidia.com/embedded/jetson-agx-xavier-developer-kit

[17] Radecki, K., Samczynski, P., Kulpa, K., & Drozdowicz, J. (2016, October). A real-time focused SAR algorithm on the Jetson TK1 board. In Image and Signal Processing for Remote Sensing XXII (Vol. 10004, p. 1000412). International Society for Optics and Photonics.

[18] P. Samczyński, Super-Convergent Velocity Estimator for an Autofocus Coherent MapDrift Technique, in IEEE Geoscience and Remote Sensing Letters, Vol. 9, Issue 2, March 2012, pp. 204-208, ISSN: 1545-598X.

[19] P. Samczyński, K. Kulpa, Coherent MapDrift Technique, IEEE Transactions on Geoscience and Remote Sensing, Vol. 48, Issue 3, 2010.

[20] K. Radecki, P. Samczyński and D. Gromek, "Fast Barycentric-Based Back Projection Algorithm for SAR Imaging," in IEEE Sensors Journal, vol. 19, no. 22, pp. 10635-10643, 15 Nov.15, 2019.